γ-ray spectroscopy of neutron-deficient ^{110}Te. II. High-spin smooth-terminating structures

E. S. Paul,[1] A. O. Evans,[1] A. J. Boston,[1] C. J. Chiara,[2,*] M. Devlin,[3,†] D. B. Fossan,[2] S. J. Freeman,[4] D. R. LaFosse,[3] G. J. Lane,[2,‡] M. J. Leddy,[4] I. Y. Lee,[5] A. O. Macchiavelli,[5] P. J. Nolan,[1] D. G. Sarantites,[3] J. M. Sears,[2] A. T. Semple,[1] J. F. Smith,[2,4,§] K. Starosta,[2,‖] A. V. Afanasjev,[6,7,8] and I. Ragnarsson[7]

[1]*Oliver Lodge Laboratory, University of Liverpool, Liverpool L69 7ZE, United Kingdom*

[2]*Department of Physics and Astronomy, State University of New York at Stony Brook, Stony Brook, New York 11794-3800, USA*

[3]*Department of Chemistry, Washington University, St. Louis, Missouri 63130, USA*

[4]*Schuster Laboratory, The University of Manchester, Brunswick Street, Manchester M13 9PL, United Kingdom*

[5]*Nuclear Science Division, Lawrence Berkeley National Laboratory, Berkeley, California 94720, USA*

[6]*Department of Physics and Astronomy, Mississippi State University, Mississippi 39762, USA*

[7]*Department of Mathematical Physics, Lund Institute of Technology, P. O. Box 118, S-22100 Lund, Sweden*

[8]*Laboratory of Radiation Physics, Institute of Solid State Physics, University of Latvia, LV 2169 Salaspils, Miera str. 31, Latvia*

(Received 12 October 2006; published 25 September 2007)

High-spin states have been populated in $^{110}_{52}$Te via ^{58}Ni(^{58}Ni,$\alpha 2p\gamma$) reactions at 240 and 250 MeV. The Gammasphere γ-ray spectrometer was used in conjunction with the Microball charged-particle detector. The high-spin ($I > 30$) collective level scheme of ^{110}Te, up to $\sim 45\hbar$, is discussed in this paper. Four new decoupled ($\Delta I = 2$) high-spin structures have been observed for the first time, together with two strongly coupled ($\Delta I = 1$) bands. These bands all show the characteristics of smooth band termination, and are discussed within the framework of the cranked Nilsson-Strutinsky approach.

DOI: 10.1103/PhysRevC.76.034323 PACS number(s): 27.60.+j, 21.10.Re, 23.20.Lv, 25.70.Hi

I. INTRODUCTION

High-spin features of the ^{110}Te nucleus beyond $30\hbar$ are documented in the present paper, while the low- and intermediate-spin structures ($I < 30$) are presented in the accompanying paper [1]. High-spin collectivity in this mass region can be induced by particle-hole (p-h) excitations, which involve the excitation of one or more $g_{9/2}$ protons across the $Z = 50$ shell gap [2,3]. With a limited number of valence nucleons available outside the ^{100}Sn closed core, conventional heavy-ion fusion-evaporation reactions can provide sufficient angular momentum to allow the observation of these level structures up to possible termination at spin $\sim$45–50$\hbar$. Such structures, originally observed in ^{109}Sb [4] have led to the concept of "smooth terminating bands" (STB) [5]. These bands have been theoretically explained as representing a slow drift of the nuclear shape from collective prolate ($\gamma \sim 0^\circ$) to noncollective oblate ($\gamma \sim 60^\circ$) over many units of spin. This interpretation has been experimentally verified following the measurement of lifetimes of levels in the $N = 58$ isotones ^{108}Sn and ^{109}Sb [6]. Similar measurements in ^{112}Te [7] have also confirmed the concept of particle-hole induced collectivity in this mass region.

Prior to this work, no evidence for collective rotational band structures was cited in ^{110}Te [8]. However, four collective $\Delta I = 2$ rotational band structures have now been observed at high spin. Two strongly coupled band structures have also been identified, as recently presented in Ref. [9]. All structures exhibit characteristics of smooth terminating bands and are interpreted using configuration-dependent cranked Nilsson-Strutinsky calculations [2,3].

II. EXPERIMENTAL DETAILS

High-spin states in the neutron-deficient nucleus ^{110}Te were populated using the ^{58}Ni(^{58}Ni,$\alpha 2p$)^{110}Te heavy-ion fusion-evaporation reaction, at a bombarding energy of 250 MeV, as detailed in Ref. [1]. In a second experiment, a target consisting of 1 mg/cm^2 of ^{58}Ni on a ^{208}Pb backing of thickness 15 mg/cm^2 was bombarded by a 240 MeV ^{58}Ni beam. The backed target was used to facilitate the measurement of mean level lifetimes using the Doppler-shift attenuation method (DSAM) [10]. Results for bands in ^{112}Te and ^{110}Te are presented in Refs. [7] and [9], respectively.

In each experiment, the Microball [11] charged-particle detector was used to select the $\alpha 2p$ channel leading to ^{110}Te and coincident γ-ray transitions were recorded with the Gammasphere [12] spectrometer; a detailed description of the data analysis is presented in Ref. [1]. Coincident γ-ray analysis was subsequently conducted with the Radware suite of graphical-analysis programs [13] in order to build a comprehensive level scheme for ^{110}Te.

[*]Present address: Department of Chemistry, Washington University, St. Louis, Missouri 63130, USA.

[†]Present address: Los Alamos National Laboratory, Los Alamos, New Mexico 87545, USA.

[‡]Present address: Department of Nuclear Physics, Research School of Physical Sciences and Engineering, Australian National University, Canberra ACT 0200, Australia.

[§]Present address: School of Engineering and Science, University of Paisley, Paisley, PA1 2BE, United Kingdom.

[‖]Present address: National Superconducting Cyclotron Laboratory, Michigan State University, East Lansing, Michigan 48824, USA.

III. EXPERIMENTAL RESULTS

The complete level scheme deduced for ^{110}Te from this work is presented in Fig. 1. The structure of levels below $I = 30$ has been discussed in detail in Ref. [1], while the high-spin results beyond $I = 30$ are discussed in this paper. Six band structures are shown in Fig. 1, labeled STB1-6. Magnetic properties of the two strongly coupled structures, labeled STB1-2, have already been discussed in Ref. [9],

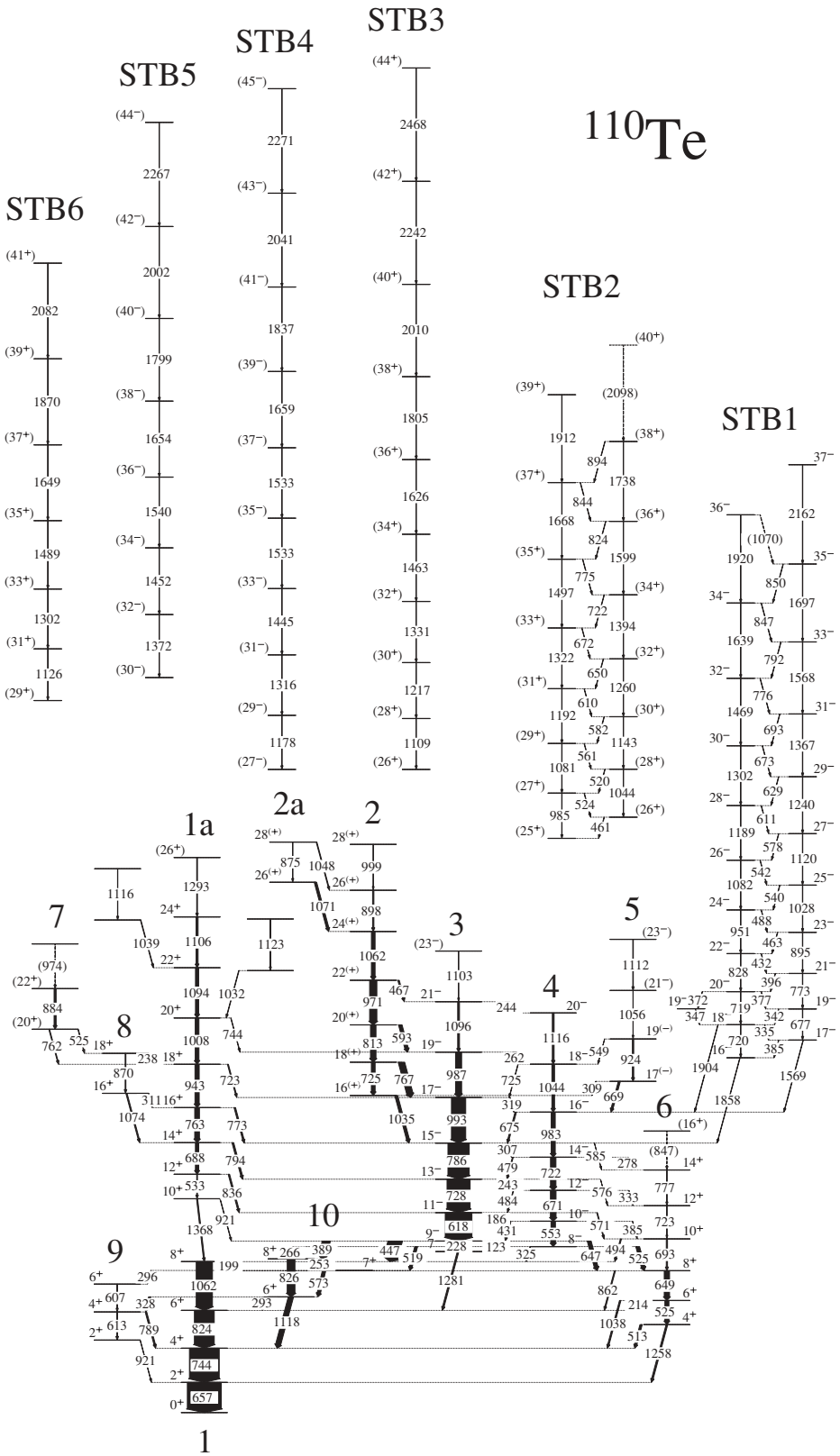

FIG. 1. The complete level scheme deduced for ^{110}Te from this work, including the high-spin smooth terminating bands, labeled STB1-6.

while STB3-6 are presented for the first time. Of the six bands presented here, only STB1 has been definitely linked into the low-spin level scheme of ^{110}Te, via three high-energy γ rays [9]. The other bands are in four-fold γ-ray coincidence with the strong low-lying transitions of ^{110}Te, although their decay paths could not be uniquely defined.

A. High-spin decoupled band structures

Four decoupled bands in ^{110}Te have been identified which extend up to high spin. Gamma-ray spectra for these bands are shown in Fig. 2, which were created from the sum of coincident double gates for all listed members of each band. Experimental results for the transitions within the bands are listed in Table I. The tentative spin-parity assignments given for STB3-6 in Fig. 1 follow from detailed comparison to theory, as discussed in Sec. IV.

TABLE I. Measured properties of the γ-ray transitions assigned to the high-spin decoupled bands in ^{110}Te.

E_γ (keV)[a]	I_γ (%)[b]
STB3	
1109.0	≡100
1216.6	82(3)
1330.7	80(3)
1463.4	64(3)
1625.5	54(3)
1805.4	38(2)
2010.0	22(2)
2242.1	8(4)
2468.2	1(1)
STB4	
1177.7	62(5)
1316.4	62(6)
1445.0	≡100
1533.0	188(7)[c]
1533.0	188(7)[c]
1658.6	92(5)
1837.3	76(5)
2041.1	36(4)
2271.1	13(2)
STB5	
1372.0	74(7)
1452.0	92(7)
1540.0	≡100
1654.0	70(6)
1799.0	46(5)
2002.0	23(4)
2267.0	9(2)
STB6	
1125.6	≡100
1302.1	99(8)
1489.0	53(5)
1649.3	64(8)
1869.8	16(4)
2082.0	<1

[a]Energies are estimated to be accurate to ±0.3 keV.
[b]Errors on relative intensities are typically ⩽5%.
[c]Intensity given for composite peak.

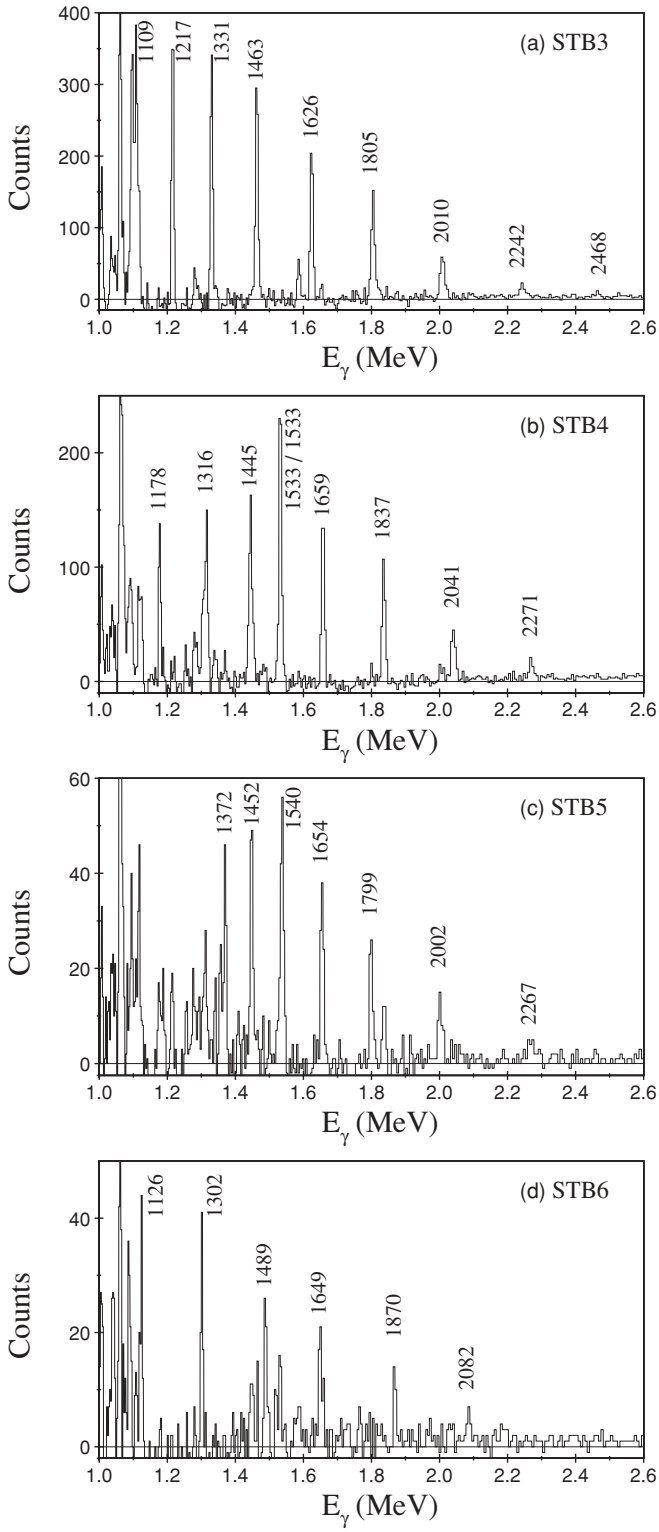

FIG. 2. Coincidence spectra generated from the sum of double gates on labeled members of the decoupled band structures, STB3–6.

STB3, illustrated in Fig. 2(a), is observed to carry ≈8% of the ^{110}Te channel intensity. It is a sequence of nine γ-ray transitions, assumed stretched $E2$ in character, increasing

in spin up to a tentative (44^+). The intensity of the γ-ray transitions is observed to decrease rapidly at high spin ($E_\gamma \geqslant$ 1805 keV), coinciding with an increase in the spacing of adjacent transitions.

STB4, shown in Fig. 2(b), was populated with a lower intensity than STB3, comprising approximately 6% of the total channel intensity. It is observed to consist of nine assumed stretched $E2$ γ-ray transitions increasing in spin up to a proposed (45^-). The intensity of the band, similar to STB3, is seen to decrease rapidly at high spin above the 1837 keV transition with the spacing between adjacent transitions increasing. Below the 1533 keV self-coincident doublet transition, intensity is observed to feed out of the band structure over the lowest three transitions of energies 1178, 1316, and 1445 keV. STB4 is seen to strongly feed band 1a and band 2, however no discrete transitions are observed carrying this intensity.

STB5, shown in Fig. 2(c), consists of seven assumed stretched $E2$ transitions increasing to a proposed tentative maximum spin of (44^-). The structure is populated with an intensity of $\approx$5% of that of the total channel intensity. STB5 shows many similarities to STB4. The band is observed to decay out over the lowest three transitions, although there is no evidence for discrete links between this structure and the low-spin level scheme.

STB6, shown in Fig. 2(d), consists of six assumed stretched $E2$ transitions, increasing in spin up to a tentative (41^+) state. The structure is populated with an intensity of $\approx$3% of that of the total channel intensity. The intensity profile of the band is similar to that of STB3, maximal at low spin, with no evidence for the intensity feeding out over several transitions. At higher spin above 1870 keV the intensity rapidly decreases as the γ-ray spacing increases. STB6 is observed to strongly feed the positive-parity structure band 1a through the structures labeled 7 and 8 in Fig. 1.

B. High-spin strongly coupled structures

Two strongly coupled band structures have been observed in ^{110}Te [9], with one connected to the low-spin level scheme via three linking transitions (see Fig. 1). Spectra for the coupled bands STB1-2 are shown in Fig. 3. Confirmation of the multipolarity of a number of transitions in STB1 was made possible following an angular correlation-analysis using the method of direction correlation from oriented states (DCO) [14]. An angular-intensity ratio,

$$R = \frac{I_{\gamma\gamma}[\theta \approx 130^\circ(50^\circ)]}{I_{\gamma\gamma}[\theta \approx 90^\circ]}, \qquad (1)$$

could be extracted, as discussed in Ref. [1], yielding values of $\sim$1.0 and $\sim$0.63, respectively, for pure stretched $\Delta I = 2$ and $\Delta I = 1$ transitions. Properties of the γ-ray transitions in STB1-2 are listed in Table II.

STB1, illustrated in Fig. 3(a), 3(b), is observed to be strongly coupled, linked by a cascade of 20 magnetic-dipole transitions. It carries $\sim$9% of the channel intensity. The intensity of the dipole transitions is observed to be at a maximum near spin (21^-). At higher spin values the reduction in intensity of the $\Delta I = 1$ transitions is offset by an increase in

TABLE II. Measured properties of the γ-ray transitions assigned to the high-spin coupled bands in ^{110}Te.

E_γ (keV)[a]	I_γ (%)[b]	R[c]	Multipolarity
	STB1		
335.3	46(3)	0.93(5)	$M1/E2$
341.8	34(3)		
346.1	21(3)		
372.3	50(3)	0.71(3)	$M1/E2$
377.3	74(3)	0.67(3)	$M1/E2$
384.6	30(3)		
396.4	$\equiv$100	0.70(3)	$M1/E2$
432.0	76(3)	0.72(3)	$M1/E2$
463.4	66(3)	0.72(3)	$M1/E2$
488.4	46(3)	0.73(3)	$M1/E2$
539.7	25(3)	0.85(6)	$M1/E2$
542.0	14(3)	0.85(6)	$M1/E2$
577.6	31(3)		
611.1	32(3)		
628.7	14(3)		
673.5[d]	38(3)		
677.0	25(3)		
692.8[e]	26(5)		
719.1[d]	66(4)		
719.9[d]	66(4)		
773.4	14(3)		
776.4[e]	13(4)		
791.6[e]	16(4)		
828.5[e]	52(6)		
847.0	7(2)		
850.0	$<$1		
895.0	27(3)		
951.4	29(3)		
1027.8	20(3)		
1070.0	$<$1		
1082.5	42(3)		
1119.5	35(3)		
1189.4	24(3)		
1239.5	20(2)		
1302.4	17(3)		
1367.0	16(2)		
1469.5	14(2)		
1567.8[e]	12(2)		
1569.2[e]	12(2)		
1638.7	8(2)		
1697.2	7(2)		
1858.4	$<$1		
1904.1	2(1)		
1920.0	$<$1		
2162.0	$<$1		
	STB2		
461.2	29(3)		
519.9[e]	150(9)		
524.1	60(3)		
560.5	$\equiv$100		
582.1	71(5)		
609.7	88(5)		
649.8[e]	122(3)		
671.6[e]	184(7)		
721.9[d]	235(11)		

TABLE II. *(Continued.)*

E_γ (keV)[a]	I_γ (%)[b]	R[c]	Multipolarity
775.2	45(5)		
824.2[d]	213(10)		
844.5	13(3)		
894.2	<1%		
985.3	10(2)		
1043.8	56(5)		
1142.5	25(2)		
1259.8	26(2)		
1394.4	15(2)		
1598.6	11(2)		
1738.4	6(2)		
2098.0	<1%		
1080.6	37(5)		
1191.5	14(2)		
1322.4	16(2)		
1497.4	16(2)		
1668.1	8(2)		
1911.5	5(2)		

[a]Energies are estimated to be accurate to ±0.3keV.
[b]Errors on relative intensities are typically ⩽5%.
[c]Ratios were obtained from the sum of gates on the 657 and 745 keV quadrupole transitions unless otherwise indicated. $R \approx 1.0$ and 0.63 represent pure stretched quadrupole and dipole transitions, respectively [1].
[d]Energy triplet: Intensity measurement is that of composite peak.
[e]Energy doublet: Intensity measurement is that of composite peak.

the $E2$ transition intensity, enabling the band to be observed to unusually high spin. Three high-energy discrete links into the low spin level scheme have been observed, of energies 1569, 1858, and 1904 keV. The 1569 keV link decays directly from (17^-) into the 16^- level of negative-parity band 4 [1]. The 1904 keV link also feeds this level from the (18^-) state, while the 1858 keV link decays from the (16^-) level into the 15^- level of negative-parity band 3 [1].

The angular-intensity ratios, R, obtained for several of the $\Delta I = 1$ transitions in STB1, are in general above the 0.63 value expected for pure dipole transitions. This implies that the transitions are of mixed $M1/E2$ character with a positive multipole mixing ratio δ, using the phase convention of Ref. [15].

STB2, illustrated in Fig. 3(c), 3(d), is observed to be strongly coupled, linked by a cascade of 13 magnetic-dipole transitions. It is populated with somewhat less intensely than STB1 (∼3% of the channel intensity). The reduction in statistics has complicated the analysis procedure and it has proved impossible to establish discrete links between this structure and the low-spin level scheme.

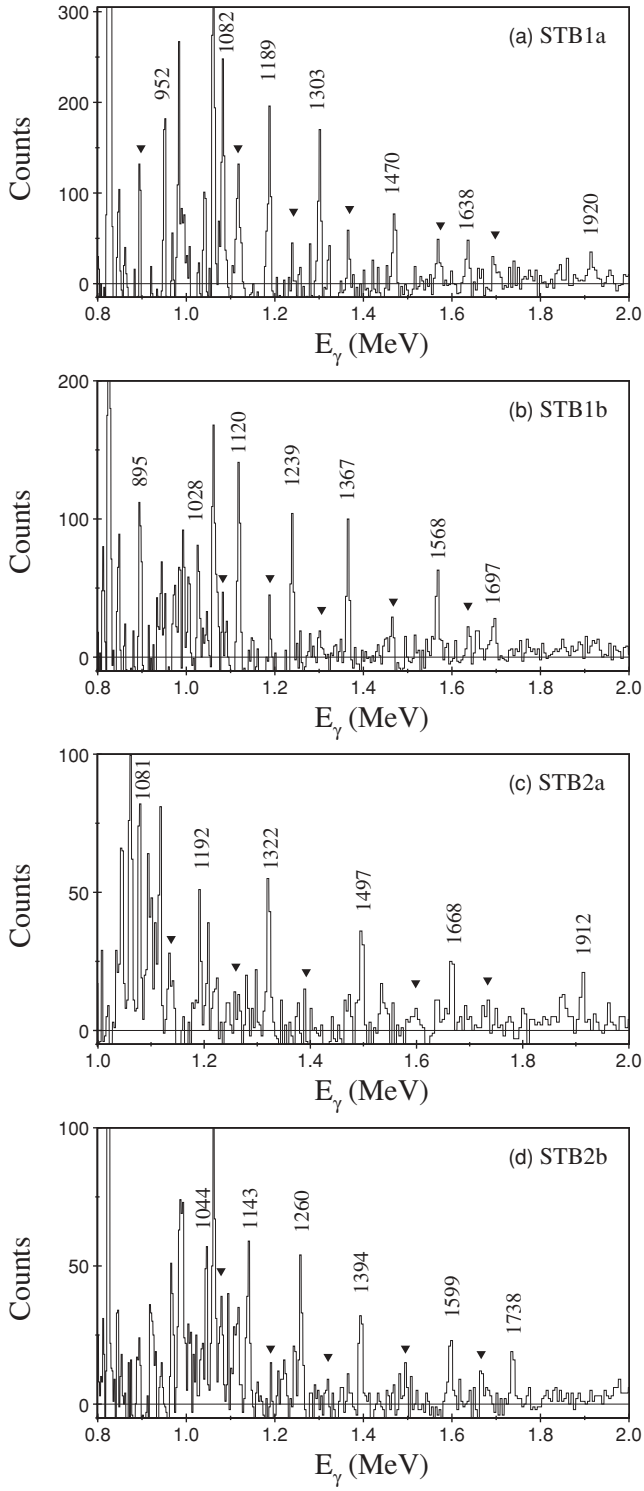

FIG. 3. Coincidence spectra generated from the sum of double gates on the two signature components of strongly coupled STB1–2. In each spectrum the triangles indicate the energies of the respective signature partner.

IV. DISCUSSION

Prior to this work, no collective high-spin structures had been observed in this nucleus. The following discussion offers an interpretation of the new results. Calculations have been performed using a configuration-dependent shell-correction approach with a cranked Nilsson potential in order to provide a theoretical interpretation of the experimentally observed band structures.

A. Smooth band termination

Nuclei near the $Z = N = 50$ doubly closed shell, such as ^{110}Te, are particularly good candidates for observing smooth terminating structures up to termination. Here only a limited number of valence nucleons are available outside of the doubly closed-shell nucleus ^{100}Sn. Therefore the angular momentum necessary to reach termination (45–50$\hbar$) for configurations with one or two holes in the $Z = 50$ core is accessible using a conventional heavy-ion fusion-evaporation reactions.

Band structures which have been understood within the framework of smooth band termination share several experimental features. One characteristic feature is a gradual decrease in the value of the dynamic moment of inertia ($\mathcal{J}^{(2)} = dI/d\omega$) to unusually low values ($\sim\mathcal{J}_{\rm rigid}/3$) with increasing rotational frequency. The $\mathcal{J}^{(2)}$ measures how transition energies change with increasing spin, therefore it is a very sensitive indicator of nuclear behavior. Fig. 4 shows a plot of the kinematic moment of inertia $\mathcal{J}^{(1)}$ ($= I/\omega$) and $\mathcal{J}^{(2)}$ as a function of rotational frequency for STB3 in ^{110}Te. The plot also shows the predicted rigid body moment of inertia $\mathcal{J}_{\rm rigid}$ corresponding to two possible values of the deformation parameter ε_2, and theoretically calculated $\mathcal{J}^{(1)}$ and $\mathcal{J}^{(2)}$ values obtained from calculations detailed in Ref. [2]. The rigid-body moment of inertia, in units of $\hbar^2$/MeV, can be simply related to a deformed nuclear shape using the expression,

$$\mathcal{J}_{\rm rigid} = 0.128A^{5/3}\,[1 + 0.29\varepsilon_2]\,. \qquad (2)$$

A value of $\varepsilon_2 = 0.135$ represents the deformation calculated using the TRS formalism [16–18] for the ground-state band in ^{110}Te, see Ref. [1]. The larger value of deformation, $\varepsilon_2 = 0.260$, is typical of a smooth terminating band at low spin. The large difference ($\mathcal{J}^{(1)} - \mathcal{J}^{(2)}$) between the kinematic and dynamic moments of inertia implies that a substantial amount of the angular momentum is generated by noncollective single-particle contributions [2], implying a terminating configuration. The experimental evidence therefore suggests that STB3 represents an example of a smooth terminating band in ^{110}Te. Furthermore, similar characteristic features are observed for all bands STB1-6 in ^{110}Te.

B. Band assignments

In order to assign specific configurations to the bands in ^{110}Te, calculations have been performed using the configuration-dependent cranked Nilsson-Strutinsky (CNS) approach [2,3,19] and using the Nilsson potential parameter set of Ref. [20]. Calculated configurations are labeled using the $[p_1 p_2, n]$ nomenclature of Ref. [2], where p_1 represents the number of $\pi g_{9/2}$ holes, p_2 represents the number of $\pi h_{11/2}$ particles, and n represents the number of $\nu h_{11/2}$ particles, relative to the $Z = N = 50$ doubly magic core. Pairing correlations are neglected in the CNS formalism.

In the following discussion, experiment and theory are presented in "rigid-rotor" plots, where energies are plotted relative to a rotating liquid-drop reference. In such diagrams, energies tend to decrease to a minimum value before increasing again for states approaching the limiting angular momentum at termination. The slopes of such plots, together with the position of the minimum energy, are highly sensitive to the spin values assigned to a band and thus may be used to assign (tentative) spin values through comparison of experiment with theory. Experimental and theoretical energies, relative to a rotating liquid-drop reference, are shown in Fig. 5 for positive-parity states and in Fig. 6 for negative-parity states.

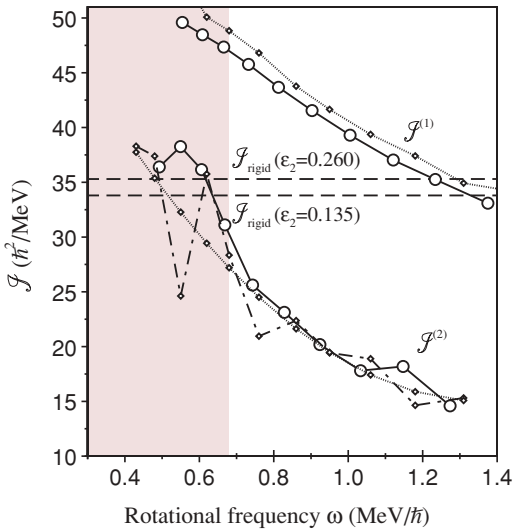

FIG. 4. (Color online) Kinematic $\mathcal{J}^{(1)}$ and dynamic $\mathcal{J}^{(2)}$ moments of inertia (open circles)extracted for STB3. The dotted lines represent theoretical $\mathcal{J}^{(1)}$ and (smoothed) $\mathcal{J}^{(2)}$ values obtained from calculations for a particular configuration (see text). The shaded area at low frequency represents the region in which pairing correlations are expected to be important.

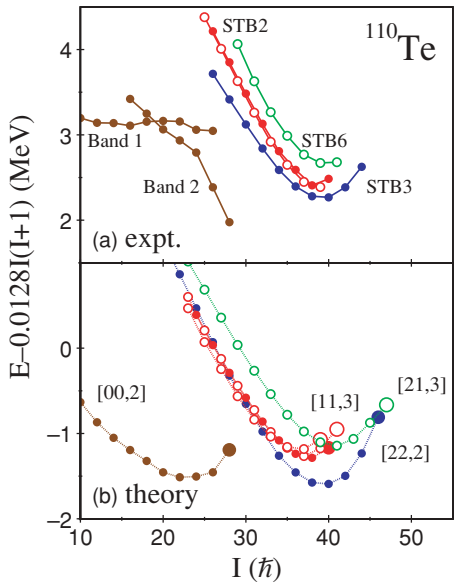

FIG. 5. (Color online) Experimental (a) and low-lying calculated bands (b) for ^{110}Te drawn relative to a rigid-rotor reference. Only positive-parity states are shown with solid circles corresponding to states with signature $\alpha = 0$ and open circles to $\alpha = 1$. Note that the relative energies of STB2, STB3, and STB6 are unknown. In (b) large symbols indicate terminating states with $\gamma = 60^\circ$.

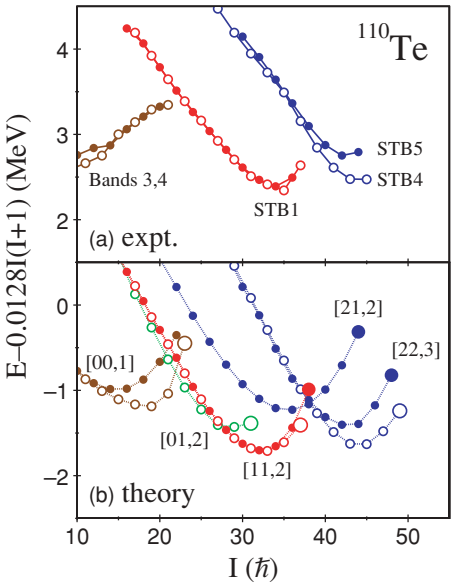

FIG. 6. (Color online) Experimental (a) and low-lying calculated bands (b) for ^{110}Te drawn relative to a rigid-rotor reference. Only negative-parity states are shown with solid circles corresponding to states with signature $\alpha = 0$ and open circles to $\alpha = 1$. Note that the relative energies of STB4, and STB5 are unknown. In (b) large symbols indicate terminating states with $\gamma = 60^\circ$.

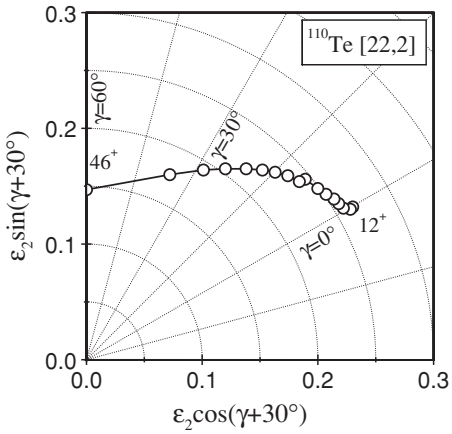

FIG. 7. Calculated shape trajectory in the (ε_2, γ) deformation plane for the [22,2] configuration. It is shown in steps of $2\hbar$ with initial and final spins indicated.

1. Decoupled stuctures

It seems plausible to associate the strongest experimental band, STB3, with the low-lying [22,2] configuration of Fig. 5. With the spins shown in Fig. 1, the experimental rigid-rotor plot of STB3 reaches a minimum at $I = 40$, in agreement with theory. STB3 continues to $I = 44$, just $2\hbar$ below the predicted terminating 46^+ state of the [22,2] configuration. The [22,2] configuration involves the 2p-2h excitation of two $g_{9/2}$ protons across the $Z = 50$ shell gap into the $h_{11/2}$ orbital. This scenario is often referred to as a core-excitation. The [22,2] configuration terminates in the state with a $\pi[(g_{9/2})_8^{-2}(h_{11/2})_{10}^2(g_{7/2}d_{5/2})_6^2]_{24} \otimes \nu[(h_{11/2})_{10}^2(g_{7/2}d_{5/2})_{12}^6]_{22}$ structure with respect to the $N = Z = 50$ closed core. The maximum spin possible with this configuration is therefore 46^+, when all the valence particles have aligned along the "rotation" axis.

Further confirmation of the [22,2] assignment is afforded with reference to the $\mathcal{J}^{(1)}$ and $\mathcal{J}^{(2)}$ plots for STB3 illustrated in Fig. 4. The theoretical values of $\mathcal{J}^{(1)}$ and $\mathcal{J}^{(2)}$ for the [22,2] configuration extracted from the calculations are overlayed on top of the experimental values. Some of the discontinuities in the theoretical moments of inertia are numerical in nature, and will be magnified in the calculations, especially for the theoretical values of $\mathcal{J}^{(2)}$. The theoretical plots therefore show the calculated values of $\mathcal{J}^{(1)}$ and a polynomial fit to the theoretical values of $\mathcal{J}^{(2)}$. The slope and magnitude of the experimental $\mathcal{J}^{(2)}$, which is a quantity independent of spin, is reproduced well by the calculations. The evolution of shape (ε_2, γ) with spin for the [22,2] configuration is shown in Fig. 7 with $\varepsilon_2 = 0.26$ at low spin ($12\hbar$) and dropping to $\varepsilon_2 = 0.14$ at termination ($46\hbar$).

It can be seen in Fig. 6(b) that theoretical signature-partner [22,3] configurations dominate at high spin above $35\hbar$. It is therefore plausible to associate STB4 and STB5 with this negative-parity configuration. The spin values shown in Fig. 1 produce the experimental rigid-rotor plots of Fig. 6(a) which match very well the theoretical [22,3] curves, in particular the slopes and position of energy minima at 42^- and 43^-. Note, however, that neither the absolute excitation energy nor the relative excitation energy of STB4 and STB5 are known. STB4 represents the second most intense high-spin terminating band in ^{110}Te and is assigned to the signature $\alpha = 1$ component of the [22,3] configuration. This configuration, which involves three $h_{11/2}$ neutrons, namely $\pi[(g_{9/2})_8^{-2}(h_{11/2})_{10}^2(g_{7/2}d_{5/2})_6^2]_{24} \otimes \nu[(h_{11/2})_{13.5}^3(g_{7/2}d_{5/2})_{11.5}^5]_{25}$, terminates at 49^-. The signature $\alpha = 0$ component of the [22,3] configuration, associated with STB5, terminates at 48^-. Corresponding bands built on the [22,3] configuration have also been assigned in ^{112}Te [7].

Finally, the weakest of the decoupled bands, namely STB6, is best described by the positive-parity [21,3] configuration of Fig. 5(b). Again, a corresponding band has been assigned in ^{112}Te [7].

From the systematic features of this mass region, see, e.g., Fig. 20 of Ref. [3], the smooth terminating $(\pi g_{9/2})^{-2}$ bands in ^{110}Te should mainly be of the type $\pi[(h_{11/2}^2)]\nu[(h_{11/2})^{2,3}]$ with $\pi[(h_{11/2})^1)]\nu[(h_{11/2})^{2,3}]$ configurations somewhat higher in energy. This is consistent with the present assignments for STB3-5. It is interesting to compare with ^{109}Sb [21] where the three lowest bands have analogous configurations as those assigned to STB3-5 in ^{110}Te with the additional proton in ^{110}Te occupying the second $h_{11/2}$ orbital. In ^{109}Sb, it was noticed [5] that the bands behave according to the spin remaining to be aligned in the configuration, $I_{\max} - I$. Similar features are seen in ^{110}Te, where the transition energies above $E_\gamma = 1600$ keV are identical to within ±20 keV in STB3-5. This fact indicates that if STB3 is observed to the $I_{\max} - 2$ state, STB4 and STB5 are observed to the $I_{\max} - 4$ state; this agrees with the above

assignments. These similarities with ^{109}Sb are an additional strong indication that the correct configurations have been assigned to these three smooth terminating bands in ^{110}Te.

2. *Strongly coupled configurations*

The two strongly coupled bands in ^{110}Te, namely STB1-2, may be considered as examples of smooth terminating dipole bands [9]. These configurations, with a single $\pi g_{9/2}$ hole in the [404]$9/2^+$ orbital, yield signature degenerate $E2$ partner bands with enhanced $M1$ strength of the interlinking dipole transitions between the partner bands. This is evident in Fig. 1 where the dipole transitions in STB1-2 are seen to energies of ~900 keV.

The stronger STB1, which has been linked into negative-parity Band 4 (see Fig. 1), naturally corresponds to the negative-parity [11,2] configuration of Fig. 6(b); this configuration is predicted to be yrast in the spin range 28–37$\hbar$. The signature-partner bands based on the [11,2] configuration terminate at spins of 37^- and 38^-, respectively. The structure of the terminating states may be written as $\pi[(g_{9/2})^{-1}_{3.5,4.5}(h_{11/2})^1_{5.5}(g_{7/2}d_{5/2})^2_6]_{15,16} \otimes \nu[(h_{11/2})^2_{10}(g_{7/2}d_{5/2})^6_{12}]_{22}$. One signature of STB1 therefore achieves termination at 37^-, while the other is just one transition away from termination at 38^-.

From the measurement of γ-ray branching ratios and mean level lifetimes, it has been possible to obtain a $B(M1)$ strength for STB1 of ~0.5 W.u. over the spin range 19–29$\hbar$, as discussed in Ref. [9]. These $B(M1)$ values remain large over an extended spin range, in contrast to the $B(M1)$ behavior found in weakly deformed $\Delta I = 1$ "magnetic" bands found in this mass region.

STB2, which is populated with a lower intensity than STB1, may be associated with a positive-parity [11,3] configuration, see Fig. 5(b). Note that the calculations predict two, almost degenerate, [11,3] configurations, which differ only by the arrangement of valence particles within the same orbitals. These [11,3] configurations are less energetically favored than the [11,2] configuration, and also lie at a higher excitation energy than the [22,2] configuration (i.e., STB3) for spins above 30$\hbar$. The signature-partner bands based on these [11,3] configurations terminate at spins of 38^+ and 39^+, or 40^+ and 41^+, respectively. With the spins shown in Fig. 1, corresponding to the rigid-rotor plot of Fig. 5(a), one signature of STB2 achieves termination at 40^+, while the other is observed to 39^+, just one transition away from termination. The structure of these terminating states may be written as $\pi[(g_{9/2})^{-1}_{3.5,4.5}(h_{11/2})^1_{5.5}(g_{7/2}d_{5/2})^2_6]_{15,16} \otimes \nu[(h_{11/2})^3_{13.5}(g_{7/2}d_{5/2})^5_{11.5}]_{25}$.

Again, it is instructive to compare with the three lowest bands in ^{109}Sb [21] where the 11 particles in the subshells above $N = Z = 50$ fill the same orbitals as discussed for the 11 particles in the decoupled structures of ^{110}Te. The only difference is then that these bands in ^{110}Te have only one $\pi g_{9/2}$ hole compared with two such holes in ^{109}Sb. Smooth terminating dipole bands based an a single $\pi g_{9/2}$ hole are extremely rare in this mass region. Indeed, apart from STB1-2 in ^{110}Te, the only other example of such structures has been found in ^{112}Te [9].

V. CONCLUSIONS

Evidence has been presented for collective structures in ^{110}Te at high spin. Four new $\Delta I = 2$ bands, in addition to two strongly coupled structures, show the characteristics of smooth band termination. Configurations have been assigned to these structures through comparison to theoretical calculations using a configuration-dependent shell-correction approach with a cranked Nilsson potential without pairing. In addition, comparisons with ^{109}Sb strengthen the assigned configurations in ^{110}Te. The structures have been shown to be based on particle-hole excitations across the $Z = 50$ shell gap. Such configurations establish a moderately deformed structure which can be traced all the way to termination into a noncollective oblate state ($\gamma = 60^\circ$).

Together with ^{112}Te [9], ^{110}Te has provided the first and only evidence, in the $A \sim 110$ region of the nuclear chart, for smooth terminating dipole bands extending to high spin. One of these structures in ^{110}Te has been linked to the low-spin level scheme, allowing confident spin-parity assignments, and is observed up to termination.

ACKNOWLEDGMENTS

This work was supported in part by the the U.K. Engineering and Physical Sciences Research Council, U.S. DOE grants DE-F05-96ER-40983, DE-FG02-07ER41459, the U.S. National Science Foundation, and the U.S. National Research Council under the Collaboration in Basic Science and Engineering Program.

[1] E. S. Paul *et al.*, Phys. Rev. C **76**, 034322 (2007).
[2] A. V. Afanasjev and I. Ragnarsson, Nucl. Phys. **A591**, 387 (1995).
[3] A. V. Afanasjev, D. B. Fossan, G. J. Lane, and I. Ragnarsson, Phys. Rep. **322**, 1 (1999).
[4] V. P. Janzen *et al.*, Phys. Rev. Lett. **72**, 1160 (1994).
[5] I. Ragnarsson, V. P. Janzen, D. B. Fossan, N. C. Schmeing, and R. Wadsworth, Phys. Rev. Lett. **74**, 3935 (1995).
[6] R. Wadsworth *et al.*, Phys. Rev. Lett. **80**, 1174 (1998).
[7] E. S. Paul *et al.*, Phys. Rev. C **75**, 014308 (2007).
[8] E. S. Paul *et al.*, Phys. Rev. C **50**, R534 (1994).
[9] A. O. Evans *et al.*, Phys. Lett. **B636**, 25 (2006).
[10] P. J. Nolan and J. F. Sharpey-Schafer, Rep. Prog. Phys. **42**, 1 (1979).
[11] D. G. Sarantites *et al.*, Nucl. Instrum. Methods A **381**, 418 (1996).
[12] I. Y. Lee *et al.*, Nucl. Phys. **A520**, 641c (1990).
[13] D. C. Radford, Nucl. Instrum. Methods A **361**, 297 (1995); **361**, 306 (1995).

[14] K. S. Krane, R. M. Steffen, and R. M. Wheeler, Nucl. Data Tables **11**, 351 (1973).
[15] T. Yamazaki, Nucl. Data A **3**, 1 (1967).
[16] W. Nazarewicz, G. A. Leander, and J. Dudek, Nucl. Phys. **A467**, 437 (1987).
[17] R. Wyss, J. Nyberg, A. Johnson, R. Bengtsson, and W. Nazarewicz, Phys. Lett. **B215**, 211 (1988).
[18] W. Nazarewicz, R. Wyss, and A. Johnson, Nucl. Phys. **A503**, 285 (1989).
[19] T. Bengtsson and I. Ragnarsson, Nucl. Phys. **A436**, 14 (1985).
[20] J. Y. Zhang, N. Xu, D. B. Fossan, Y. Liang, R. Ma, and E. S. Paul, Phys. Rev. C **39**, 714 (1989).
[21] H. Schnare *et al*., Phys. Rev. C **54**, 1598 (1996).